



SPACE VECTOR AND SIGNAL PROCESSING FOR VOLTAGE DIPS MONITORING

Pierre Granjon¹, Seddik Bacha² and Vanya Ignatova²

¹: Gipsa-lab, Département Images Signal, CNRS, INPG

²: G2Elab, Equipe SYREL, CNRS, INPG

Contact author: pierre.granjon@gipsa-lab.inpg.fr

Abstract: A new method for voltage dips monitoring in power networks is presented in this paper. This method is based on the space vector representation, which is a time-dependent complex-valued quantity equivalent to the original three-phase voltages. In the case of non-faulted system voltages, the space vector follows a circle in the complex plane with a radius equal to the nominal voltage. This shape becomes an ellipse in the case of voltage dip, with parameters depending on the phase(s) in drop, dip magnitude and phase angle shift. The parameters of the space vector shape are determined by classical signal processing tools and are used to determine the dip time period, classify and finally characterize the measured power quality disturbance. Algorithms are detailed for each step of this automatic method and are validated on real measurement data.

Keywords: power networks, power quality monitoring, voltage dips, three-phase transforms, signal processing.

1. INTRODUCTION

The power networks area undergoes constant technical and economical modifications due to the power market deregulation. Because of these new considerations power quality monitoring has become of major concern. Voltage dips are the most common types of power quality disturbances. Moreover, they lead to important economical losses and/or distorted quality of industrial products. Indeed, equipments have become more sensitive to such phenomena as a result of technology improvement and increased use of power electronics devices (Anderson and Nilson, 2002; McGranaghan *et al.*, 1993). Thus, voltage dips monitoring has become an essential requirement for power quality monitoring.

The final objective of this work is to elaborate a method able to automatically detect and characterize measured voltage dips, and localize the original fault inside the monitored power network. However, this paper only deals with the first two points (dip detection and characterization), and can be viewed as the first step of this global project.

Three-phase voltage dips being the most frequent power quality disturbance, main research interests are focused on their analysis. The time duration where the dip occurs is determined by segmentation algorithms applied to the three-phase voltages independently (Styvaktakis, 2002). The dip signature can be identified from voltage waveforms (Bollen and Zhang, 2003), from the comparison between RMS values of phase voltages and phase-to-phase voltages (Bollen and Styvaktakis, 2000), or well from symmetrical components (Bollen and Zhang, 2006). However, each of these techniques see the three-phase measurement as three different dimensional

quantities, and process each phase voltage independently, which is far from being optimal.

In this paper, a new method for voltage dips analysis is developed. It is based on the space vector transform which merges the original three-phase measurements into an equivalent mono-dimensional complex-valued quantity called the space vector. This quantity can then be further analyzed by using signal processing tools in order to automatically detect and characterize measured voltage dips.

This paper is organized as follows: Section II deals with voltage dips signatures as a function of fault type and location, system grounding and monitor's connection; Section III describes the space vector transformation and its representation in the complex plane in case of voltage dips. Algorithms for dips segmentation, classification and characterization are presented in section IV, and illustrated with measurement data in section V.

2. VOLTAGE DIPS

In power networks, voltage dips are defined as short-duration reductions in voltage magnitude at the fundamental frequency. They are generated by phase to ground or phase to phase faults that occur at one point of the network. Voltage dips propagate through the network, and can be observed at different locations thanks to voltage sensors. An observed voltage dip is characterized by its duration, magnitude and phase angle shift on each phase of the network. The last two parameters completely determine the dip type, also called "dip signature". Obviously, a dip signature depends on power network parameters (system grounding, presence of transformers in the propagation path, connections of monitor, ...), on the

measurement location, and on fault characteristics (fault type and location in the power network). Fig. 1 represents the most usual voltage dips signatures based on the so-called ABC classification (Bollen, 1999). In this figure, each signature (from A to G) is represented by the complex voltages of each phase a , b , and c at the fundamental frequency of the network.

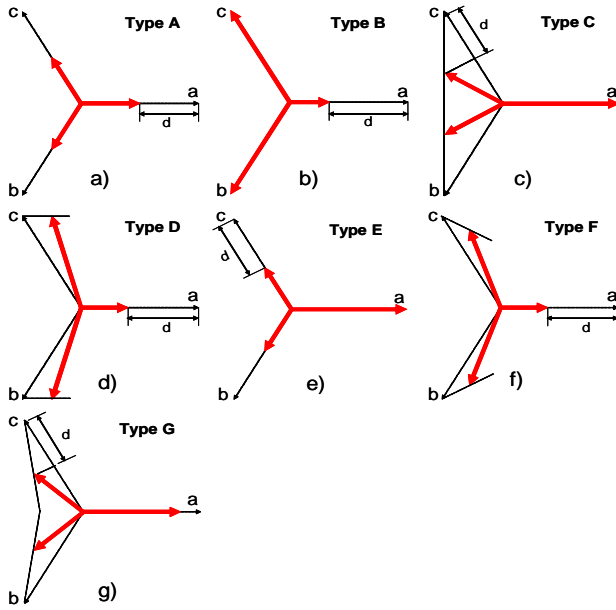


Fig. 1. Most usual voltage dip signatures.

Type B, D and F voltage dips are characterized with a major drop in one of the phases, and are called single phase voltage dips. Type C, E and G are characterized with major drops in two of the phases and are called double phase dips. The dip type A is called three phase dip. It has been shown (Zhang, 1999) that power network transformers usually remove the zero-sequence voltage, defined as the sum of the three line voltages. Hence, only type A, C, D, F and G, which have a null zero-sequence voltage, will be considered in the following.

The aim of the next sections is to describe a new simple and powerful method able to detect, classify and characterize potential voltage dips signatures at one point of a monitored network. This method should be considered as the first step of a power network monitoring system. But first, the three-phase voltage measurement has to be simplified by cleverly using a classical three-phase transformation.

3. SPACE VECTOR AND VOLTAGE DIPS

In this work, the measured quantities are three line voltages at one location of the monitored power network. Under mild conditions, this time-dependent real-valued three-phase quantity can be transformed into the complex-valued mono-dimensional space vector. This section theoretically defines this last quantity, and shows that the parameters of its shape in the complex plane depend on the dip signature.

3.1 Space vector origin and definition.

Symmetrical components have been first introduced by Fortescue in 1918 in order to analyse a sinusoidal three-phase quantity. Later, Lyon generalized this concept by applying it to time-dependant real- or complex-valued three-phase quantities, independently of their waveform. This general transformation, applied to a three-phase system $x_a(t)$, $x_b(t)$ and $x_c(t)$, can be expressed under the following matrix form:

$$\begin{pmatrix} x_d(t) \\ x_i(t) \\ x_0(t) \end{pmatrix} = \frac{2}{3} \begin{pmatrix} 1 & a & a^2 \\ 1 & a^2 & a \\ \frac{1}{2} & \frac{1}{2} & \frac{1}{2} \end{pmatrix} \begin{pmatrix} x_a(t) \\ x_b(t) \\ x_c(t) \end{pmatrix}, \quad (1)$$

where $a = e^{j2\pi/3}$.

By analogy with Fortescue's symmetrical components, the transformed components $x_d(t)$, $x_i(t)$ and $x_0(t)$ are called the direct-, indirect- and zero-sequence component, respectively. Together, they form the instantaneous symmetrical components. In our case, the nature of the measurements induces several simplifications. First, the analyzed three-phase system is constituted by real-valued line voltages noted $v_a(t)$, $v_b(t)$ and $v_c(t)$. The corresponding direct- and indirect-sequence components $v_d(t)$ and $v_i(t)$ are then complex conjugated, and are completely equivalent. Second, the zero-sequence voltage $v_0(t)$ is supposed to be removed by one or several transformers present in the monitored power network. Under these assumptions, all the information contained in the original three-phase system $v_a(t)$, $v_b(t)$ and $v_c(t)$ is contained in the direct-sequence component $v_d(t)$. For sake of simplicity, this quantity is noted $v(t)$ in the following, and is calculated thanks to Eq. (2):

$$v(t) = \frac{2}{3} [v_a(t) + av_b(t) + a^2v_c(t)]. \quad (2)$$

Finally, it can be noted that under the previous assumptions, Eq. (2) transforms a three dimensional real quantity $(v_a(t), v_b(t), v_c(t))$ into a mono dimensional complex-valued one $(v(t))$. This equivalent quantity, also called "space vector" in the literature, can be easily analysed thanks to classical signal processing tools as shown in the next sections.

3.2 First harmonic approximation.

In terms of first harmonic, line voltages can be viewed as sinusoidal quantities before, during and after the fault. Then, they can be represented by using Euler's formula as the sum of two contra rotating complex components, with angular frequency $\pm 2\pi f_0$ rad/s (f_0 is the power network fundamental frequency). For example, the line voltage of phase a can be written as:

$$v_a(t) = V_a \cos(2\pi f_0 t + \phi_a) = \frac{V_a}{2} \left(e^{j(2\pi f_0 t + \phi_a)} + e^{-j(2\pi f_0 t + \phi_a)} \right).$$

The space vector, derived from the previous expression reported in Eq. (2), becomes a sum of one positive and one negative angular frequency component:

$$v(t) = V_p e^{j2\pi f_0 t} + V_n e^{-j2\pi f_0 t}, \quad (3)$$

where $V_p = |V_p| e^{j\angle V_p}$ and $V_n = |V_n| e^{j\angle V_n}$ are complex numbers depending on line voltages magnitude and phase.

From Eq. (3), it follows that the space vector represented in the complex plane rotates around the origin at the angular frequency $\pm 2\pi f_0$, and follows an ellipse shape as shown in Fig. 2. Major axis r_{maj} , minor axis r_{min} and inclination angle ϕ of this ellipse depend on V_p and V_n (Bachschmid *et al.*, 2004):

$$\begin{aligned} r_{maj} &= |V_p| + |V_n| \\ r_{min} &= \left| |V_p| - |V_n| \right| \\ \phi &= \frac{\angle V_p + \angle V_n}{2} \end{aligned} \quad (4)$$

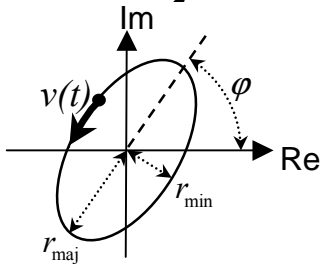


Fig. 2. First harmonic space vector approximation in the complex plane.

In order to easily characterize the shape followed by the space vector in the complex plane, a shape index SI is introduced as follows:

$$SI = \frac{r_{min}}{r_{maj}} = \frac{\left| |V_p| - |V_n| \right|}{|V_p| + |V_n|}. \quad (5)$$

Its value ranges from 0 to 1, and can be interpreted as the correlation coefficient between the space vector shape and a perfect circle:

- if $SI = 1$, $v(t)$ follows a circle shape,
- if $0 < SI < 1$, $v(t)$ follows an ellipse shape,
- if $SI = 0$, $v(t)$ follows a straight line.

3.3 Space vector in case of voltage dips.

Voltage dips lead to changes in the form followed by the space vector in the complex plane. The form parameters (SI , r_{min} , r_{maj} and ϕ) are determined in this paragraph as a function of the dip type.

Flawless case. In a balanced sinusoidal three phase system, the three line voltages have the same

magnitude and their relative phase angle shift is $\frac{2\pi}{3}$.

Then, the space vector is only composed of a positive angular frequency component, and follows a circle in the complex plane, with radius equal to the nominal voltage V . In that case, its analytic expression is given by $v(t) = V e^{j(2\pi f_0 t + \phi)}$.

Single phase voltage dips. Single phase dip types considered here are type D and F. It has been shown in (Ignatova *et al.*, 2005) that their space vector is composed of positive and negative angular frequency components and follows an ellipse shape in the complex plane. The characteristics of this ellipse are given in Table 1, where d corresponds to the dip depth defined in Fig. 1, and $n=1, 2, 3$ denotes the phase affected by the fault.

Table 1 Single phase voltage dips.

Dip type	Space vector shape characteristics			
	SI	ϕ	r_{min}	r_{maj}
D	$1-d$	$\frac{\pi}{2} + (1-n)\frac{\pi}{3}$	$(1-d)V$	V
F	$\frac{3(1-d)}{3-d}$	$\frac{\pi}{2} + (1-n)\frac{\pi}{3}$	$(1-d)V$	$\left(1-\frac{d}{3}\right)V$

It can be noted that r_{min} is directly linked to the dip depth d and can be used to detect such dips. Once detected, the differentiation between these two single phase dips can be done thanks to r_{maj} , which is different in these two cases. Finally, the inclination angle ϕ is used to determine which phase is subject to major drop: $\phi = \frac{\pi}{2}$ for phase a , $\phi = \frac{\pi}{6}$ for phase b and $\phi = -\frac{\pi}{6}$ for phase c . This last point is illustrated in Fig. 3.

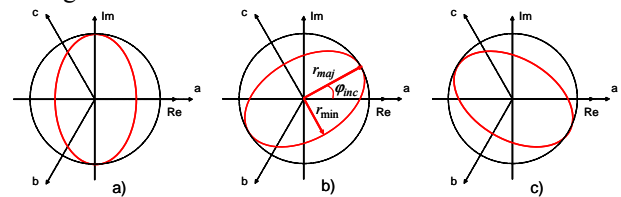


Fig. 3. Space vector shape for a single phase dip type D on phase a , b and c respectively.

Double phase voltage dips. In the same way, the shape followed by the space vector in the complex plane can be used to analyze double phase voltage dips. Table 2 gives the shape parameters in case of dip types C and G, where d still denotes the dip depth, but n is now the phase not affected by the fault.

Once again, the ellipse minor axis r_{min} allows to detect these dips, its major axis r_{maj} allows to determine the dip type (C or G), and its inclination

angle φ gives the phases affected by the dip: phase a if $\varphi = 0$, b if $\varphi = -\frac{\pi}{3}$ and c if $\varphi = \frac{\pi}{3}$.

Table 2 Double phase voltage dips.

Dip type	Space vector shape characteristics			
	SI	φ	r_{\min}	r_{\max}
C	$1 - \frac{4}{3}d$	$(1-n)\frac{\pi}{3}$	$(1 - \frac{4}{3}d)V$	V
G	$\frac{5-6d}{5-2d}$	$(1-n)\frac{\pi}{3}$	$(1 - \frac{6}{5}d)V$	$(1 - \frac{2}{5}d)V$

Three phase voltage dips. In this case, the space vector is only composed of one positive frequency component as in the non-faulted case, but with a smaller magnitude: $v(t) = (1-d)V e^{j(2\pi f_0 t + \varphi_0)}$. It follows a circle shape ($SI=1$), with a radius depending on the dip severity ($r_{\min} = r_{\max} = (1-d)V$). This dip characteristics are presented in Table 3.

Table 3 Three phase voltage dips.

Dip type	Space vector shape characteristics			
	SI	φ	r_{\min}	r_{\max}
A	1	-	$(1-d)V$	$(1-d)V$

This section shows that in terms of first harmonic, the space vector follows an ellipse shape which parameters (SI , r_{\min} , r_{\max} and φ) depend on the type of voltage dips at the measurement point. All these parameters have been determined with respect to the dip type, and are given in Tables 1, 2 and 3. These results are used in the following in order to analyze (detect, identify and characterize) potential voltage dips.

4. VOLTAGE DIPS ANALYSIS METHOD

The previous results are used in this section in order to develop a voltage dips analysis method. Its general structure depicted in Fig. 4, is detailed in the following.

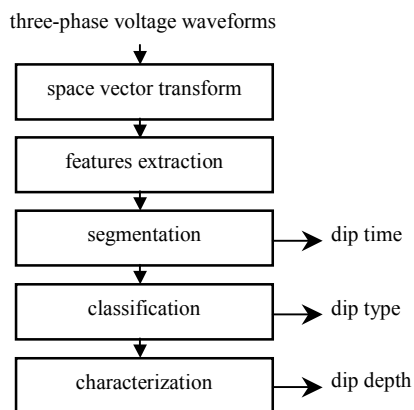


Fig. 4. Steps for dips analysis method

4.1 Space vector transform.

This instantaneous transformation is defined by Eq. (2). Under the previous assumptions, the output of this first step is the space vector $v(t)$, a mono-dimensional complex-valued quantity completely equivalent to the original three-phase (three-dimensional) voltage system. In this case the general expression of $v(t)$, given by Eq. (3), is a sum of two complex exponentials with frequency $\pm f_0$ and complex amplitude V_p and V_n .

4.2 Features extraction.

The aim of this second step to extract the main characteristics of the shape followed by the space vector $v(t)$ in the complex plane. Section 3 shows that this shape is an ellipse, completely defined by its major and minor axes r_{\max} and r_{\min} , its shape index SI and its inclination angle φ (see Fig. 2). Moreover, Eq. (4) and (5) show that these characteristics only depend on complex amplitudes V_p and V_n . Therefore, the aim becomes to correctly estimate V_p and V_n from the space vector $v(t)$ given by Eq. (3). This is exactly the role of the Fourier transform, which analyzes complex waveforms by means of complex exponentials. Finally, the so-called Short-Time Fourier Transform (STFT) will be used in order to follow the time evolution of V_p and V_n , and hence of r_{\max} , r_{\min} , SI and φ . The length of the STFT time window corresponds to one fundamental period of the power network (20 ms) in order to correctly describe the space vector shape while precisely following its time evolution.

A simple example is given in Fig. 5 through a measured dip voltage. Fig. 5a represents a three-phase voltage measured at one point of a power network, which undergoes a strong voltage dip after 0.04 seconds. During this dip, the space vector follows an ellipse shape, represented in the complex plane in Fig. 5b during one fundamental period. The corresponding amplitude spectrum is represented in Fig. 5c, where two strong components at ± 50 Hz are easily localized. These components correspond to the complex exponentials defined in Eq. (3). Therefore, the complex amplitudes V_p and V_n can be easily determined from this Fourier Transform, and hence the different shape parameters r_{\max} , r_{\min} , SI and φ .

It should be noted that measured voltages are often disturbed by noise or harmonics, and the corresponding space vector shape is not always a perfect ellipse (see for example Fig. 5). However, the use of the Fourier Transform minimizes the negative impact of such disturbances since it is perfectly adapted to the estimation of complex exponential parameters.

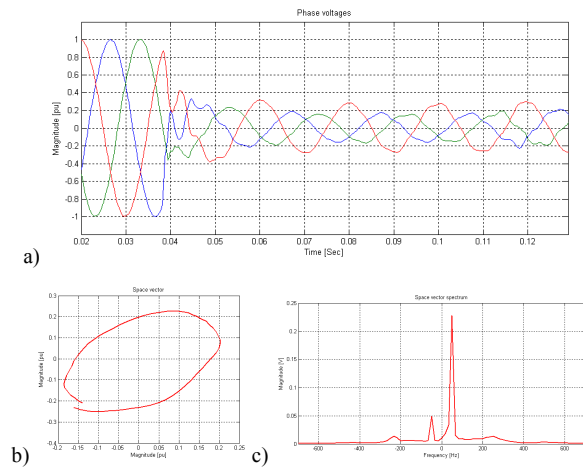


Fig. 5. Measured voltage dip (a), corresponding space vector shape in the complex plane (b), and space vector spectrum (c).

4.3 Segmentation.

The segmentation process refers to the decomposition of a given signal into stationary or weakly non stationary segments. In the case of three-phase voltage dips, one segmentation algorithm is usually applied to each of the three phases, because the phases in change are not known *a priori*. Afterwards, the results obtained on each phase have to be merged in order to take a global segmentation decision on the recorded waveforms (Bollen, 1999).

In our case, Tables 1, 2 and 3 show that when a dip occurs, the dip depth d increases and the ellipse minor axis r_{\min} becomes smaller than the nominal voltage V . Hence, a unique segmentation algorithm can be applied on r_{\min} to determine the dip time period by detecting changes in its mean value. In this work, the segmentation algorithm is a change in the mean Cusum (Cumulative Sum) algorithm, chosen for its good performance, great simplicity and optimal properties (Basseville and Nikiforov, 1993). This algorithm automatically determines different segments during which r_{\min} can be considered has a constant. The mean value of r_{\min} is estimated by averaging on each segment, and compared to a threshold of $0.9V$ in order to determine the segments where voltage dips occur.

4.4 Classification.

The previous step automatically determines the different time segments where voltage dips occur. The present one has to establish which type of dip occurs during each of these segments. Therefore, we suppose in this paragraph that a dip has been detected during the current segment.

Tables 1, 2 and 3 indicates that the ellipse shape index SI , inclination angle φ , and major axis r_{maj} can be used to discriminate different voltage dip types. SI is first used in order to differentiate unbalanced dips (single or double phase dips) from balanced ones (three-phase dips). The limit value of SI is calculated

for a dip depth equal to 10% of the nominal voltage and is set to 0.93 (see Table 1 and 2 with $d = 0.1$). Then, if SI is greater than 0.93, the dip is automatically classified to type A (three-phase voltage dip). On the contrary if SI is lower than 0.93, the dip can be single or double phase. Then, φ determines whether the dip is single or double phase, and indicates the phase(s) with major drop (see Tables 1 and 2 again). This result is illustrated in Fig. 6, where single phase dips are denoted with S, double phase dips with D, and phase(s) in drop are in lower case letters.

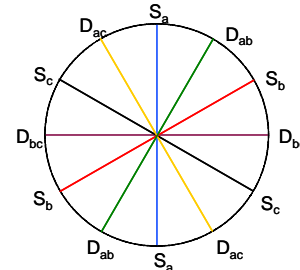


Fig. 6. Unbalanced dip classification thanks to the ellipse inclination angle.

Finally, r_{maj} contribute to the complete dip classification by differentiating dip types with the same ellipse inclination (discrimination between D and F, and between C and G).

4.5 Characterization.

Once the dip type determined, it can be useful to evaluate its severity, represented by the dip depth d , previously defined in Fig. 1. Tables 1, 2 and 3 shows that if the dip type is known, the ellipse minor axis value r_{\min} allows to determine the dip depth d .

In the next section, the performance of this method is evaluated by applying it to three-phase voltages measured at one point of a power network.

5. APPLICATIONS

The previous method has been implemented with Matlab. Its performance is illustrated in this section through results obtained with data measured on a medium voltage network. Only dips with duration over one cycle are analyzed. Phase voltages and space vector characteristics are given in p.u. with respect to the nominal voltage V .

The proposed method is applied to the recorded voltage waveforms presented in Fig. 7a. The space vector is first calculated from the voltage measurements, and the STFT over one cycle is applied to this complex quantity. From these short time spectra, the time evolution of r_{maj} , r_{\min} , SI and φ are determined and represented in Fig. 7 (r_{maj} and r_{\min} in Fig. 7b, φ in Fig. 7c). These results are the output of the features extraction step of the proposed method.

Next, the segmentation algorithm detects a voltage dip between 0.04 and 0.15 seconds by analysing the evolution of r_{\min} , which is below the threshold of 0.9 p.u. (see Fig. 7b). All curves of Fig. 7 are bold during this period.

During the dip, the shape index SI decreases until 0.6 and the corresponding dip is classified as unbalanced. Moreover, the ellipse inclination angle φ stays near 180° (red bold markers in Fig. 7c), which indicates a double phase voltage dip (type C or G), with phases b and c in drop (see Fig. 6). The ellipse major axis $r_{\text{maj}} = 0.85$ is clearly lower than 1, and finalizes the classification step with a dip type set to G (see Table 2).

Finally, the ellipse minor axis being $r_{\min} = 0.5$ p.u., the characterization step evaluates the dip depth at approximately $d = 0.41$ p.u..

This result seems to be coherent with voltage waveforms of Fig. 7, where it can be seen that two phases are mainly in drop (double phase dip), and their drop is around 0.4 p.u..

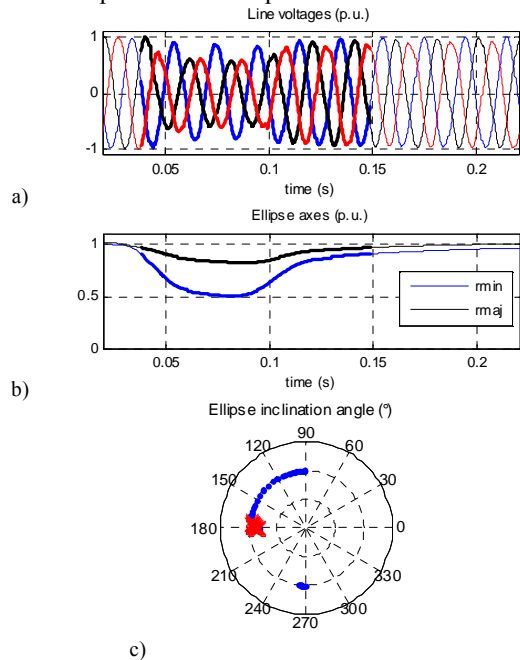


Fig. 7. Double phase voltage dip (a), corresponding ellipse axes (b), and inclination angle φ (c).

6. CONCLUSION AND FUTURE WORKS

In this paper, a new method for voltage dips analysis is developed. It is based on the analysis of the space vector, a mono-dimensional complex-valued quantity containing the same information as the original three-phase voltage system under mild assumptions. The shape characteristics of this quantity, extracted thanks to signal processing tools, allows to detect, classify and characterize potential three-phase voltage dips.

The different examples shows that this method reaches good performance, even in the presence of wide band noise and/or harmonic distortion. Furthermore, the proposed method could be easily real-time implemented in view of on-line power

quality monitoring, since it relies on very simple algorithms (instantaneous space vector transform, STFT, change in the mean Cusum-type algorithm).

Two main directions can be further explored in future works. First, this method has to be generalized in order to classify all the dip types presented in section II. In such a general method, the zero-sequence voltage may be different from zero and has to be taken into account. In that case, a complex quantity such as the space vector is not sufficient to completely characterize the voltage dips, but a quaternionic quantity could do the job. It should also be noted that in that case, the signal processing tools used to analyze this quantity must be adapted.

The second direction concerns the localization of the fault which generated the measured voltage dip. Such information may be determined thanks to the joint analysis of the three-phase voltages and currents.

REFERENCES

- Andersson T., and D. Nilsson (2002), *Test and evaluation of voltage dip immunity*, STRI report, Sweden.
- Bachschmid N., P. Pennacchi and A. Vania (2004), *Diagnostic significance of orbit shape analysis and its application to improve machine fault detection*, J. Braz. Soc. Mech. Sci. & Eng., vol.26 no.2 Rio de Janeiro.
- Basseville M., and I. Nikiforov (1993), *Detection of Abrupt Changes. - Theory and Application*, Prentice-Hall.
- Bollen M., (1999), *Understanding Power Quality Problems : Voltage Sags and Interruptions*, Wiley-IEEE Press.
- Bollen M., and L. Zhang (1999), *A method for characterization of three phase unbalanced dips from recorded voltage waveshapes*, IEEE Telecommunication Energy Conference.
- Bollen M., and S. Styvaktakis (2000), *“Characterization of Three-phase Unbalanced Sags, as easy as one, two, three”*, IEEE PES Summer Meeting 2000, Seattle, WA, USA.
- Bollen M., and L. Zhang (2003), *Different methods for classification of three-phase unbalanced voltage dips due to faults*, Electric Power Systems Research, Vol. 66, no.1, pp.59-69.
- Ignatova V., P. Granjon, S. Bacha and F. Dumas (2005), *Classification and characterization of three phase voltage dips by space vector methodology*, FPS conference.
- McGranaghan M., D. Mueller and M. Samotyj (1993), *Voltage sags in industrial systems*, IEEE Transactions on industry applications, Vol. 29, No.2, pp. 397-403.
- Styvaktakis E., (2002), *Automating power quality analysis*, Ph.D. thesis., Chalmers University of Technology, Sweden.
- Zhang L., (1999), *Three-phase unbalance of voltage dips*, Licentiate thesis, Chalmers University of Technology, Dept Electric Power Engineering, Gothenburg, Sweden.